Environmental Science and Ecotechnology 24 (2025) 100538

Contents lists available at ScienceDirect

Environmental Science and Ecotechnology

journal homepage: www.journals.elsevier.com/environmental-science-and-ecotechnology/

Original Research

Urban fabric decoded: High-precision building material identification via deep learning and remote sensing

Kun Sun [a], Qiaoxuan Li [b], Qiance Liu [a, c], Jinchao Song [a], Menglin Dai [c], Xingjian Qian [d, e], Srinivasa Raghavendra Bhuvan Gummidi [a], Bailang Yu [d, e], Felix Creutzig [f, g, h], Gang Liu [c, i, *]

[a] SDU Life Cycle Engineering, Department of Green Technology, University of Southern Denmark, Odense, 5230, Denmark
[b] School of Resources and Environmental Science, Quanzhou Normal University, Quanzhou, 362000, China
[c] College of Urban and Environmental Sciences, Peking University, Beijing, 100871, China
[d] Key Laboratory of Geographic Information Science, Ministry of Education, East China Normal University, Shanghai, 200241, China
[e] School of Geographic Sciences, East China Normal University, Shanghai, 200241, China
[f] Mercator Research Institute on Global Commons and Climate Change, EUREF 19, Berlin, 10829, Germany
[g] Bennett Institute for Innovation and Policy Acceleration, University of Sussex Business School, Brighton, BN1 9SL, UK
[h] Technical University Berlin, Straßedes 17 Junis 135, Berlin, 10623, Germany
[i] Institute of Carbon Neutrality, Peking University, Beijing, 100871, China

A R T I C L E I N F O

Article history:
Received 27 June 2024
Received in revised form
26 January 2025
Accepted 26 January 2025

Keywords:
Building material intensity
Built environment
Streetview image
Remote sensing
Deep learning

A B S T R A C T

Precise identification and categorization of building materials are essential for informing strategies related to embodied carbon reduction, building retrofitting, and circularity in urban environments. However, existing building material databases are typically limited to individual projects or specific geographic areas, offering only approximate assessments. Acquiring large-scale and precise material data is hindered by inadequate records and financial constraints. Here, we introduce a novel automated framework that harnesses recent advances in sensing technology and deep learning to identify roof and facade materials using remote sensing data and Google Street View imagery. The model was initially trained and validated on Odense's comprehensive dataset and then extended to characterize building materials across Danish urban landscapes, including Copenhagen, Aarhus, and Aalborg. Our approach demonstrates the model's scalability and adaptability to different geographic contexts and architectural styles, providing high-resolution insights into material distribution across diverse building types and cities. These findings are pivotal for informing sustainable urban planning, revising building codes to lower carbon emissions, and optimizing retrofitting efforts to meet contemporary standards for energy efficiency and emission reductions.

1. Introduction

As a substantial global energy consumer and carbon dioxide emitter, the construction industry is pivotal in addressing climate change and achieving ambitious global targets for carbon neutrality [1–3]. The International Energy Agency (IEA) estimates that the building sector was responsible for approximately one-third of worldwide energy- and process-related CO_2 emissions in 2021. It encompasses 8% of direct emissions, predominantly from building operations, 19% attributed to electricity and heat used in buildings, and 6% from the production and transport of construction materials [4]. The persistent upward trend in energy use and emissions, rebounding to pre-pandemic levels [5,6], underscores the urgent need for decarbonizing the building sector [7,8]. To this end, the precise identification and categorization of materials used in existing buildings are critical, yet often unavailable, for informing embodied carbon reduction, building retrofitting, and circularity strategies for buildings and cities [9,10].

Typically, the consumption of building materials in existing structures is represented by material intensity, indicating the

* Corresponding author. College of Urban and Environmental Sciences, Peking University, Beijing, 100871, China.
E-mail address: gangliu@pku.edu.cn (G. Liu).

https://doi.org/10.1016/j.ese.2025.100538
2666-4984/

number of materials used per unit area or volume. Material intensity coefficients are derived from official construction documents, standards, or public statistics records [11,12]. The sources, while valuable, often offer only a partial view, focusing on individual projects or specific geographic areas [13,14]. Alternatives, such as estimates derived from demolishing data, provide sporadic insights but lack consistency for comprehensive analysis [15,16]. The challenges [17,18] in standardizing material intensity coefficients are further exacerbated by the diverse influences of local contexts, such as cultural, technological, and regulatory factors on building practices [19]. For example, a global building material intensity database [20], which contains around 300 samples from 21 nations, covers mostly developed European regions and cannot adequately represent the global building characteristics, which consist of over a billion structures [21,22]. Efforts to incorporate more regional data from countries like China [23], Denmark [24], the Netherlands [25], the Philippines [26], Canada [27], and others [28] continue, yet the process is still labor-intensive and slow [29]. Moreover, the varied methods used to classify buildings based on their materials, purposes, and specifications complicate the creation of a universally applicable database [30,31]. The ongoing challenges related to data availability, methodological consistency, model interpretability, and large dataset management underscore the need for innovative approaches in building material-intensity research.

Recent advancements in optical and satellite-based sensing technologies have revolutionized acquiring high-quality, high-resolution street views and remote sensing images, significantly benefiting the construction industry and urban management [32,33]. These technologies support primary data collection and enable detailed analysis of building structures [34,35]. For example, high-resolution imagery aids in precise building footprint extraction [36] and roof material identification [37], which is crucial for urban sustainability projects. Moreover, state-of-the-art research in remote sensing has explored innovative approaches for building uses and aging through advanced image analysis [38], significantly enhancing real-time urban planning and decision-making processes [39]. Cutting-edge cases illustrate the depth of urban analysis possible with modern remote sensing, from building assessment to evaluating urban sustainability [40,41].

Despite the abovementioned capabilities, variability in data collection and analysis methods often hinders the widespread adoption of interpretative methodologies [42,43]. Deep learning has significantly enhanced remote sensing applications by enabling complex, high-dimensional data processing, particularly in identification and semantic segmentation tasks [44–46]. Recent studies have leveraged models like Convolutional Neural Networks (CNNs), U-Net, and attention mechanisms to address inefficiency and instability in traditional processing [47]. Innovations in semantic segmentation and classification tasks have enhanced the ability to capture spatial context more effectively by implementing advanced backbones and multi-scale feature extraction. For instance, FarSeg++ further improves segmentation accuracy in complex backgrounds by incorporating foreground-aware optimization and context modeling [48]. Furthermore, deep learning provides tools to standardize urban data analysis, transforming vast information into actionable insights for urban sustainability [49]. Researchers have increasingly applied deep learning to decouple urban fabric, leveraging high-dimensional data such as street views to deconstruct urban elements [50]. The processes have enabled advancements in analyzing building age [39,51], type [52,53], façade materials [54], economic factors [55], and material usage [56].

By leveraging remote sensing data and deep learning techniques, this study seeks to refine the process of identifying and classifying building materials, specifically focusing on exterior walls and roofs. The innovative framework enhances the accuracy and efficiency of detecting materials and introduces a novel method for determining new material intensity coefficients based on the identified material categories. The dual approach contributes to the construction industry by improving the assessment of material usage and reducing buildings' carbon footprint through more accurate analysis. While initially implemented and tested in four major Danish cities, the framework has been extended to other urban settings in Denmark, demonstrating its potential applicability and scalability.

2. Materials and methods

2.1. Description of data sources and dataset construction

This study combines Google Street View (GSV) and satellite imageries supplemented by OpenStreetMap (OSM) geospatial data. The geospatial data include building location and road networks, essential for accurately locating each building in the corresponding visual images. Fig. 1 showcases the elements, illustrating the roof structures and textures from satellite images (Fig. 1b), as well as façade textures from GSV (Fig. 1c and d). The dual-source approach allows for a comprehensive analysis of urban structures' vertical and horizontal aspects.

The retrieval process is initiated by extracting building geographic coordinates (latitude and longitude) from OSM. The coordinates are crucial as they locate the buildings precisely within GSV and Google satellite platforms. Python scripts complete the fetching of street-level and satellite images, ensuring each image is accurately matched to the corresponding building. Detailed steps for obtaining Street View imagery and preprocessing the initial data can be found in the Supplementary Materials. The foundational dataset is primarily sourced from Odense, which has well-documented geospatial data and diverse architectural styles. To assess the model's broader applicability and regional adaptability, we extrapolated functions to include building data from other major Danish cities, such as Copenhagen, Aarhus, and Aalborg. The expansion demonstrates the model's capability to generalize across different urban settings without needing localized adjustment. The datasets are divided into subsets for training, validation, and testing according to standard machine-learning protocols, supporting the

Fig. 1. Illustration of geospatial and visual data fusion for building material classification. The figure integrates geospatial with visual data to classify building materials effectively. **a**, An aerial view of the targeted building outlined by a white dashed rectangle, providing context within its surrounding environment. **b**, The roof of the building, utilizing satellite imagery to analyze roofing materials. **c**–**d**, Front (**c**) and side (**d**) perspectives of the building's façade, as captured by Google Street View for classifying wall materials. These images, retrieved using precise geographic coordinates from OpenStreetMap, ensure accurate alignment and are instrumental in comprehensively analyzing the building materials.

rigorous phases of model training and evaluation. Fig. 2 provides a composite visualization of datasets, showcasing selections of outwall materials from GSV and roof materials from the satellite imagery, underscoring the data's diversity and detail.

2.2. Workflow for building instance categorization using Google Street View and satellite images

The methodology for categorizing building materials leverages high-resolution data from GSV and satellite imagery (Fig. 3). Utilizing Python 3.8 for scripting and ArcGIS 10.2 for geospatial visualization, this study begins by retrieving the building footprints and road network from OpenStreetMap. Concurrently, façade materials are analyzed using street-level imagery obtained through Google Application Programming Interfaces (APIs), while roof materials are assessed from satellite imagery. The street view images undergo preprocessing with a pre-trained VGG16 model trained on the Places2 dataset [57] to filter out non-building elements, such as trees and fences, that could obscure material features. Images are then labeled according to the type of materials documented, encompassing various roof and façade materials. The CNN models, including Densenet and Efficientnet, are utilized to classify materials based on the unique characteristics captured in the imagery.

Multi-category construction data from Odense, the 3rd largest city chosen for its diverse representation of Danish building materials and well-documented geospatial dataset, serves as the training dataset for the study. Detailed descriptions of the dataset composition and its use in training and evaluation are provided in Supplementary Material Section 4. Separate modeling and forecasting are conducted for street view data and remote sensing images. 20% of the original dataset is utilized as an independent test set to ascertain the models' accuracy. The performances of thirteen state-of-the-art CNN models were evaluated through precision and reliability measures to select the most effective approach for deployment, and all models were pre-trained on the heterogeneous ImageNet dataset to enhance generalization and convergence. The transfer learning method has proven to improve model performance across various computer vision tasks.

The entire workflow, from data collection to model evaluation, is designed to optimize the accuracy and applicability of classification frameworks in diverse urban environments. The adaptability and thoroughness of methods are demonstrated by the city-scale distribution maps of building materials derived from the model outputs. The distribution maps provide essential insights for urban planning and sustainability, illustrating the practical application of classification systems across varied settings.

2.3. Model visualization and interpretation techniques

Several advanced visualization techniques were incorporated to bolster deep learning models' interpretability in categorizing building materials. The techniques demystify the opaque operations of deep learning models by revealing the inner decision-making processes and highlighting critical points.

- **Gradient-weighted Class Activation Mapping (Grad-CAM)**: Grad-CAM [58] generates a heatmap by computing the gradients of any target concept, capturing the specific feature map activations that contribute to the final decision. When overlaid on the original image, the heatmap accentuates the region with the most influence on the model's predictions. Notably, Grad-CAM operates without modifying the neural network structure, maintaining the model's original integrity while providing profound insights.
- **Guided Backpropagation**: This approach [59] enhances traditional backpropagation by exclusively propagating positive gradients and activations. The selective propagation amplifies the visibility of critical features such as textures and edges, enriching the understanding of visual processing. It is particularly effective in scrutinizing how models respond to different image textures, which is pivotal for assessing building material types.
- **Guided Grad-CAM**: Combining the advantages of Grad-CAM and Guided Backpropagation, Guided Grad-CAM [60] refines the initial coarse heatmaps. Calculating positive gradients linked to ultimate predictions within the feature maps pinpoints crucial image regions with heightened accuracy. Guided Grad-CAM prevents the potential misguidance from global information that might affect Guided Backpropagation alone.

Together, the visualization tools enhance the neural network's transparency and interpretability. By offering a more granular and focused examination of the model's operations on specific tasks, they facilitate more informed decision-making, leading to better material choices, improved maintenance strategies, and more sustainable urban environments.

2.4. Estimation of material intensity based on aggregate building data

Buildings are classified based on the materials used in their walls and roofs, drawing from previous studies [24,61] that contain detailed architectural and material data. The classification allows for analyzing material usage patterns across different building types. The specific material intensity is calculated by dividing the total mass of materials used by the total floor area for a given building type, providing a normalized matrix of material consumption. The material intensity coefficient represents the average material usage per square meter and is crucial for assessing the sustainability of building practices. The formula used for the processing is as follows:

$$\mathit{Material\ intensity}_{material,type} = \frac{\sum\left(\mathit{Total\ weight\ of\ specific\ material}_{type}\right)}{\sum \mathit{Total\ floor\ area}_{type}} \tag{1}$$

where *material* refers to the specific building material (e.g., concrete, timber), and *type* denotes the building category based on wall and roof materials.

3. Results and discussion

3.1. Classification model performance and interpretability

The performances of the thirteen state-of-the-art CNN models on multi-category tasks are displayed in Fig. 4a–c. The performance of the models in predicting building façade materials using street view images varies significantly. The variation in model performance can be attributed to the complex background elements in the outwall database, which may impede accurate classification. Hence, analyzing and comparing model performance under comparable settings is essential for making an informed model selection. Based on the performance distribution depicted in Fig. 4a and Supplementary Material Table S2, Shufflenet achieved the highest global prediction accuracy at 78.6% for façade material classification. In comparison, Resnet50 excelled in roof material classification with an overall accuracy of around 80%. Detailed recall, precision, and F1 scores for each model can be found in

Fig. 2. Composite visualization of outwall and roof materials from multi-source imagery in datasets. **a**, A selection of outwall material samples from Google Street View. **b**, Corresponding roof material samples retrieved from Google satellite based on geographic coordinates. PVC, polyvinyl chloride.

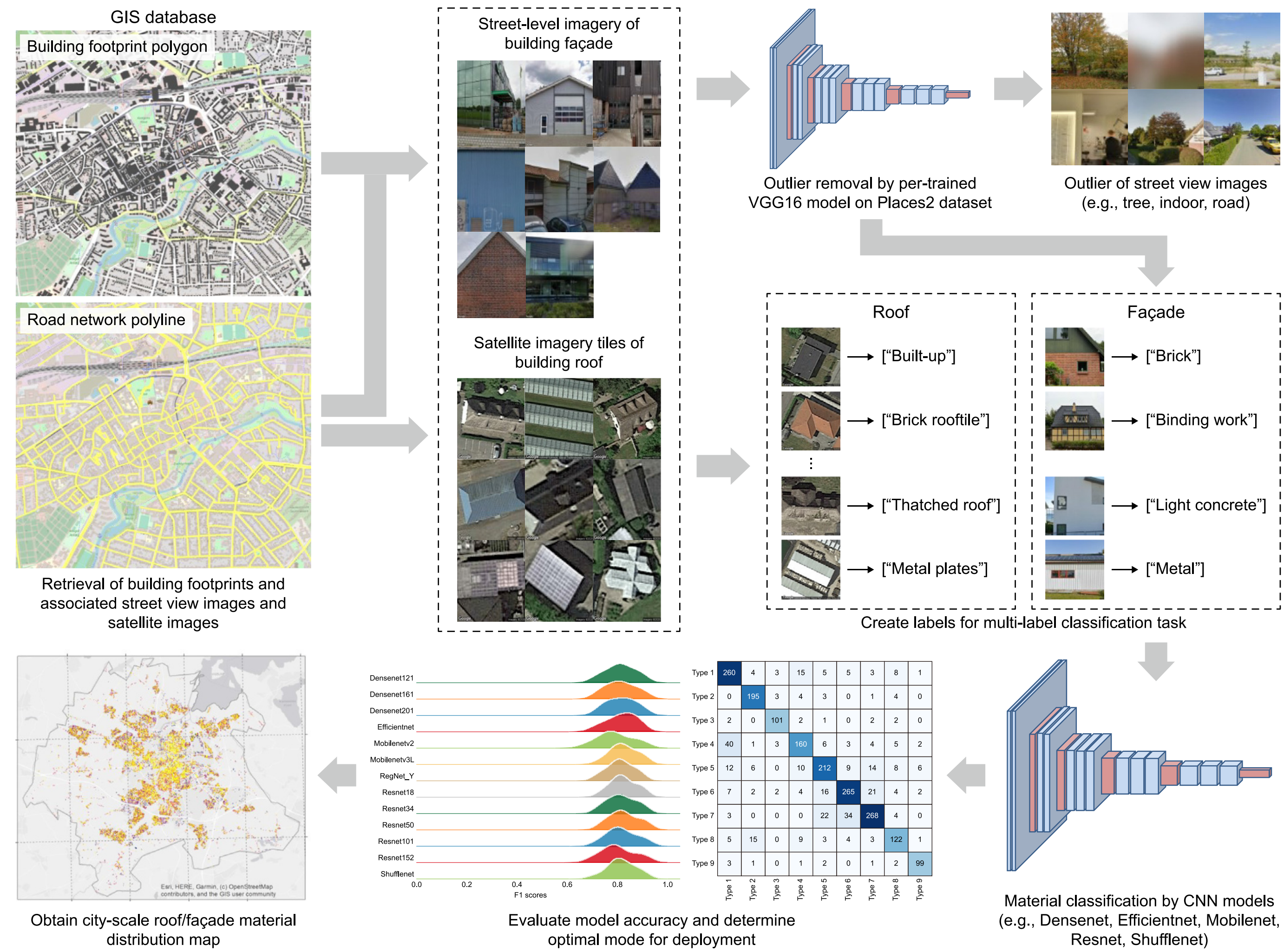

Fig. 3. A dual-model approach for urban building material classification based on deep learning and multi-source imageries. The workflow begins with collecting geospatial data and corresponding imagery and filtering out non-building elements. Advanced Convolutional Neural Networks are trained for roof and façade material classification and rigorously evaluated for performance. The optimal models, selected for their robustness, are applied to assess material in different urban settings. GIS, Geographic Information System.

Supplementary Materials Tables S2 and S3.

As illustrated in Fig. 5, the techniques reveal how specific regions of an image contribute to the model's predictions, with warmer areas indicating higher relevance. Grad-CAM helps localize key informative components of the image, enhancing the precision of forecasts by highlighting areas critical to the model's decision-making. Understanding how different elements like window types or decorating materials influence models' predictions can guide architects and urban planners to align better with sustainability goals or regulatory requirements. Guided Backpropagation emphasizes the influence of each pixel during the output generation process, preserving the original image's details, which aids in understanding the model's feature utilization. Guided Backpropagation allows researchers to visually observe specific image features, such as lines, edges, or texture patterns. Researchers can enhance classification accuracy by precisely detecting the distinct surface textures of various building materials, such as bricks, stone, and metal plates. Simultaneously, nuanced alterations in texture can also contribute to evaluating and monitoring the building conditions, including assessing the signs of wear or damage to their visual looks. These characteristics are crucial for upholding the security of structures and conserving historical sites. Combining contextual highlights of Grad-CAM with the detail-oriented focus of Guided Backpropagation, Guided Grad-CAM provides a composite view that accentuates critical features while diminishing background noise, clearly depicting how combined textual and contextual information guides the model's predictions. The visualization tools are indispensable for dissecting complex deep-learning models, offering insights into potential misclassifications, and facilitating model optimization. Enhancing the transparency of decision-making processes within models enables researchers and engineers to refine and implement deep learning algorithms more efficiently, augmenting their interpretability and utility in practical applications.

3.2. Model generalization across geographic regions

Fig. 6 showcases city-scale classification maps for roofing and façade materials across Aarhus, Odense, Copenhagen, and Aalborg. The maps utilize a color-coded system to denote different materials, demonstrating the model's ability to generalize across varied urban landscapes. The visualization helps highlight the distinct architectural styles and material usage that characterize each city, reflecting how regional building practices adapt to local environmental and socioeconomic conditions. The detailed exploration of roofing materials is extended in Supplementary Materials

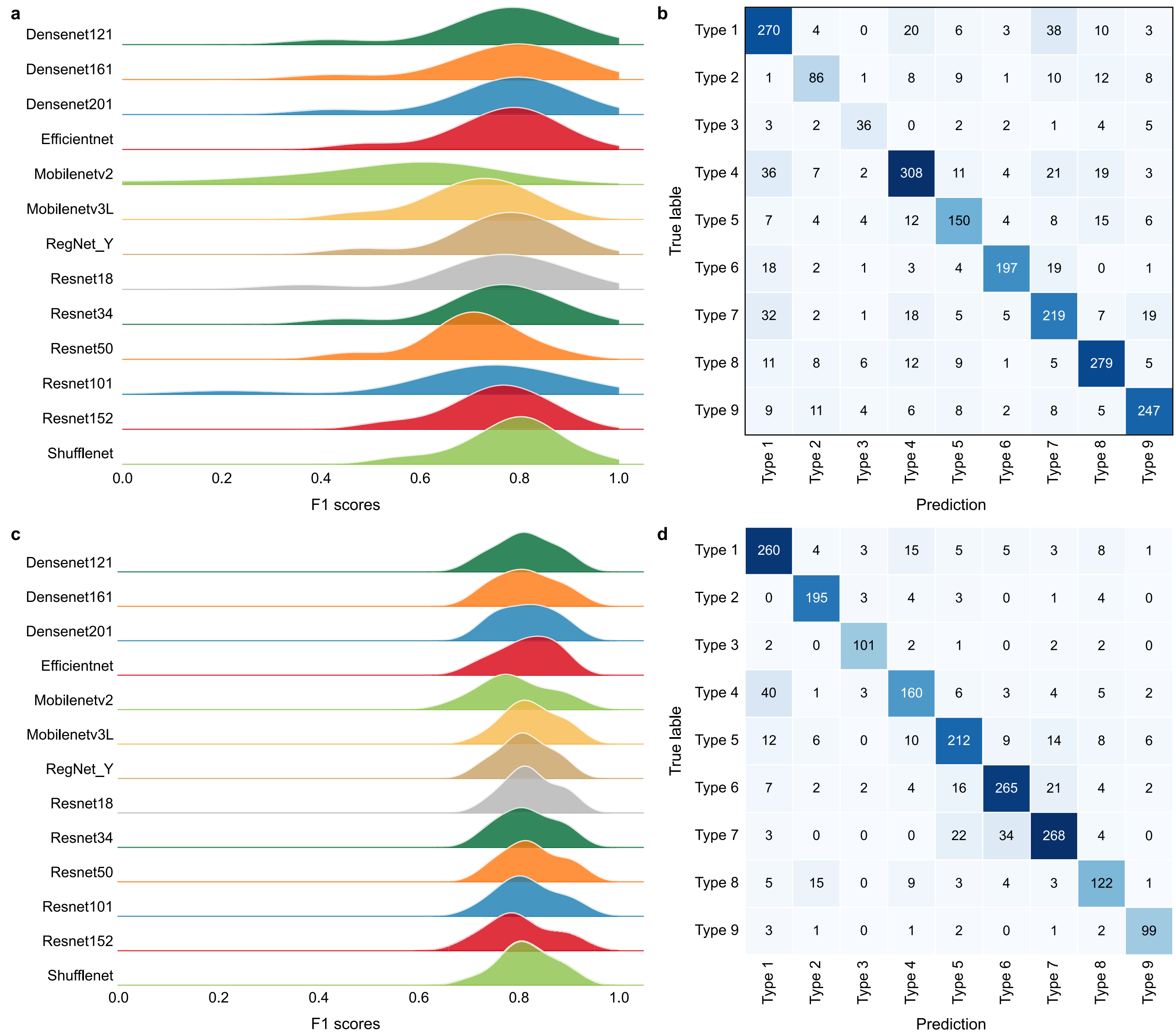

Fig. 4. Performance analysis of deep learning models in building material classification. **a**, F1 score distributions for different models in outwall material identification, where the F1 score illustrates the models' stability and robustness across categories. **b**, Matching matrix of Shufflenet for outwall identification, highlighting the model's predictive accuracy and misclassifications. **c**, F1 score distribution for models classifying roof materials, comparing model efficacy. **d**, The accuracy matrix for Resnet50 in roof material classification shows the proportion of correctly and incorrectly classified instances. The specific material types are defined in Table S4 (Supplementary Material), which assists in interpreting the material classification designations.

Figs. S5–S8. The supplementary figures offer a deeper dive into the specific roofing materials prevalent in each city, enhancing our understanding of the architectural diversity. For instance, Supplementary Materials Figs. S5–S8 detail how different materials are distributed across cityscapes, revealing patterns such as the prevalence of metal roofing in the industrial zones of Aarhus and the dominance of cement roofing in the commercial centers of Copenhagen. The patterns underscore the adaptability of the deep learning model and enrich our insights into how construction materials are influenced by local factors such as climate, history, and urban planning policies.

Similarly, the façade material classification results are elaborated upon in Supplementary Materials Figs. S9–S12. The figures provide a granular view of how façade materials vary across the urban core to the periphery of each city, offering a nuanced perspective on the interaction between architectural design and urban environment. For example, the prevalence of brick facades in the historical centers contrasts with the modern materials found in the newer developments, illustrating the dynamic evolution of urban facades in response to changing architectural trends and building technologies. Integrating detailed mappings and analyses, our study demonstrates the robust generalization capabilities of the deep learning model and provides a valuable tool for urban planners and architects. The model's ability to accurately classify and analyze building materials on a city-wide scale supports sustainable urban development and aids in designing cities that harmonize historical heritage with modern design. This cohesive narrative highlights the model's technical performance and

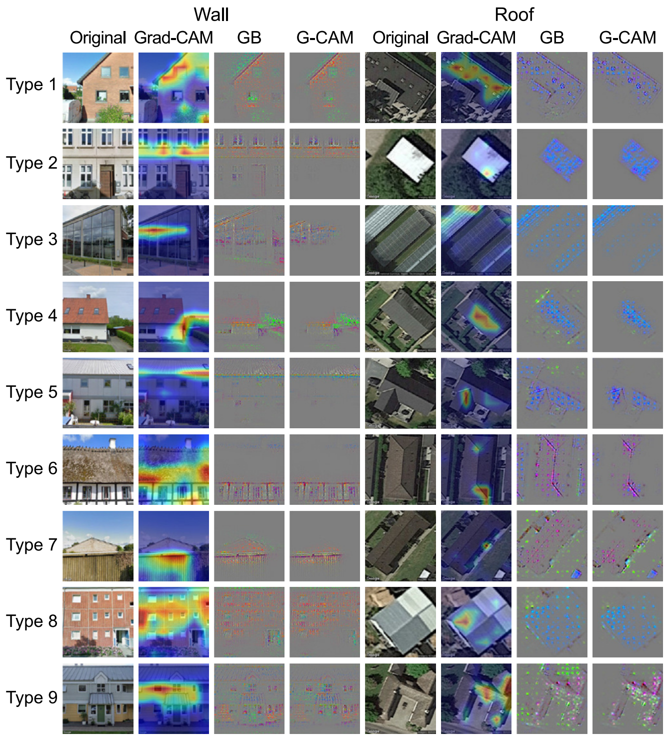

Fig. 5. Comparative visualizations of model predictive focus for material classification. Columns display original images alongside their Gradient-weighted Class Activation Mapping (Grad-CAM) heatmaps indicating predictive regions, Guided Backpropagation (GB) detailing pixel importance, and Guided Grad-CAM (G-CAM) merging both approaches to highlight critical features influencing model decisions.

practical applications, offering a comprehensive view of material classification across major Danish cities.

3.3. Material intensity across different construction types

We have calculated and evaluated residential and non-residential buildings' material intensity coefficients (MIC) in detail based on several reliable data sources [24,62,63]. The analysis reveals the patterns in materials used across different wall and roof combinations, highlighting their environmental impact and sustainability implications. Fig. 7 visualizes the patterns for residential buildings through heat maps of MICs. Certain combinations, such as built-up roofs (Type 1, average MIC: ~1326 kg m^{-2}) and polyvinyl chloride (PVC) roofs (Type 2, average MIC: ~1588 kg m^{-2}), exhibit consistently lower MIC across various wall types, indicating higher material efficiency and environmental friendliness. In contrast, combinations involving cement stone roofs (Type 6) with binding work walls yield significantly higher coefficients (2225 kg m^{-2}), reflecting greater material consumption and environmental impact. While combinations involving glass walls (Type 3) and fiber cement with asbestos (Type 5) roofs exhibit moderate coefficients (1730 kg m^{-2}), suggesting a trade-off between structural integrity and material efficiency, it is noted that using asbestos in construction has significantly declined in recent decades due to its associated health risks. A comprehensive evaluation of the combinations should also consider environmental impact, potential health hazards from legacy materials, and the cost-effectiveness of modern substitutes. Moreover, by analyzing the distribution of specific materials and their associated construction techniques, in combination with building construction years, it is possible to estimate the likely decommissioning timelines for buildings. The information can provide valuable insights for urban mining initiatives, enabling better planning for material recovery and reuse in specific regions.

Wall construction generally plays a more significant role in material intensity than roof construction. For instance, binding work walls (Type 6) exhibit the highest average material intensity (2215 kg m^{-2}), indicative of dense, material-intensive construction methods. Thatched roofs (Type 9) stand out among roofing materials with higher average coefficients (1861 kg m^{-2}), likely due to substantial material demands or intricate installation requirements. While aesthetically appealing and beneficial for natural lighting, glass roofs necessitate robust supporting structures due to their weight and environmental load considerations. Heatmaps for non-residential buildings, presented in Fig. S13, align with the trends observed in residential buildings. The insights underscore the critical role of material selection in promoting sustainability and balancing functional and aesthetic needs with ecological considerations.

3.4. Implications for urban sustainability and generalization of the proposed methods

As global urbanization intensifies and the global population grows, urban sustainability emerges as a pressing concern for modern society [64]. World Bank data indicates that more than 50% of the people currently reside in urban areas, accounting for over 80% of the global gross domestic product [65]. Rapid urbanization is accompanied by substantial land, resource, and energy consumption. Existing urban buildings, major contributors to global energy consumption and waste generation, nonetheless present significant opportunities for sustainable development. Effective management and retrofitting can enhance energy efficiency, reduce emissions, and elevate regional architectural and environmental standards. However, implementing tailored retrofit strategies across diverse regions and building types is challenging and often hindered by limited data availability. Only a few developed areas, such as Manchester [12], Vienna [66], Melbourne [67], and Padua [14], possess comprehensive cadastral data to support such strategies. Therefore, pursuing urban sustainability in comparatively underdeveloped regions or lacking historical documentation necessitates adopting a large-scale, cost-efficient assessment technique to address data deficiencies. Remote sensing technology offers a swift and economical solution for characterizing urban landscapes. Combined with geospatial data, for example, collected in the EUBUCCO database [68], it enables the rapid estimation of building location, size, age, surrounding environment, and energy efficiency. Evaluating building material intensity requires distinguishing between building functions and ages, ideally supported by building material compilation databases, such as the previously compiled global building material intensity databases for 21 countries [20] and 32 regions [28].

This study introduces a novel methodological framework for assessing building material intensity by focusing on identifying rooftop and exterior wall materials through remote sensing and deep learning techniques. The exposed materials are key indicators of buildings' structural composition and significantly influence their environmental impact. By accurately characterizing building materials, the framework enables the development of region-specific material intensity databases tailored to different areas' unique building archetypes and preferences. The proposed approach leverages the efficiency and accessibility of remote sensing and street view data to overcome the limitations of traditional data collection methods, which often suffer from incompleteness and inaccuracies. The framework can infer the underlying material composition by analyzing the spectral signatures of the

Fig. 6. **a**–**d**, The city-scale roofing classification maps of Arhus (**a**), Odense (**b**), Copenhagen (**c**), and Aalborg (**d**). The maps synthesize the results of the optimal deep learning model applied to roof images of all urban buildings, with counts of 43,476, 84,542, 59,767, and 85,902, respectively. Each building is represented by a color-coded point based on the classified roofing material, with the scale of data indicating near-complete urban coverage. **e**–**h**, Detailed predicted urban façade material distribution maps of Arhus (**e**), Odense (**f**), Copenhagen (**g**), and Aalborg (**h**), denoting each material with a color-coded marker derived from 18,571, 31,695, 26,928, and 23,916 building images, respectively. The disparity in image volumes is attributed to data unavailability and variable image quality.

rooftop and exterior wall materials, providing valuable insights into embodied energy and carbon footprints. Furthermore, identifying the materials used allows for recommending environmentally responsible replacements during renovations or retrofits. Considering thermal performance, weight, and overall sustainability, decision-makers can select optimal materials to enhance energy efficiency and reduce environmental impacts. Additionally, material combinations can help determine building energy consumption standards, aiding urban planners in making informed decisions.

However, there are limitations to the current study, such as sampling frequency, data quality, and resolution, which can affect the reliability of the material assessments. Future work will focus on incorporating additional data sources, including Light Detection and Ranging (LiDAR) and oblique photography, to improve the accuracy and comprehensiveness of material identification. Detailed building information is crucial for decision-makers involved in urban planning, building renovation, and policy development. By understanding the material intensity of existing building stock, stakeholders can make well-informed decisions about the material selections for new constructions and retrofits, prioritizing sustainable and low-carbon alternatives. Moreover, precise material understanding enables the evaluation of building-related carbon emissions, aiding efficient strategies to mitigate climate change. This knowledge assists policymakers and construction professionals pinpoint high-energy-consuming buildings, allowing for specific upgrades to maximize energy conservation efforts.

4. Conclusion

This study advances the methodology for identifying construction materials through remote sensing and deep learning. It addresses a crucial gap in urban management by providing a granular understanding of material distribution, benefiting decision-makers in comprehending construction practices' material demands and environmental impacts. The insights inform policies promoting sustainable spatial planning, resource management, enhanced building codes, and optimized retrofitting. The methodology's adaptability ensures its applicability across diverse locations and architectural styles, supporting sustainable urban development. However, limitations exist, such as potential inaccuracies if exterior walls or roofs have undergone modifications and the inability to identify interior structures. Future research should explore incorporating additional data sources like building information modeling, lidar, oblique photography, and construction drawings for a more comprehensive assessment. A multi-scale building performance assessment approach can be established by addressing these limitations and expanding applications to other project management domains. This thorough analysis, combined with interdisciplinary collaborations and the integration of advanced technologies, will bolster building energy efficiency and

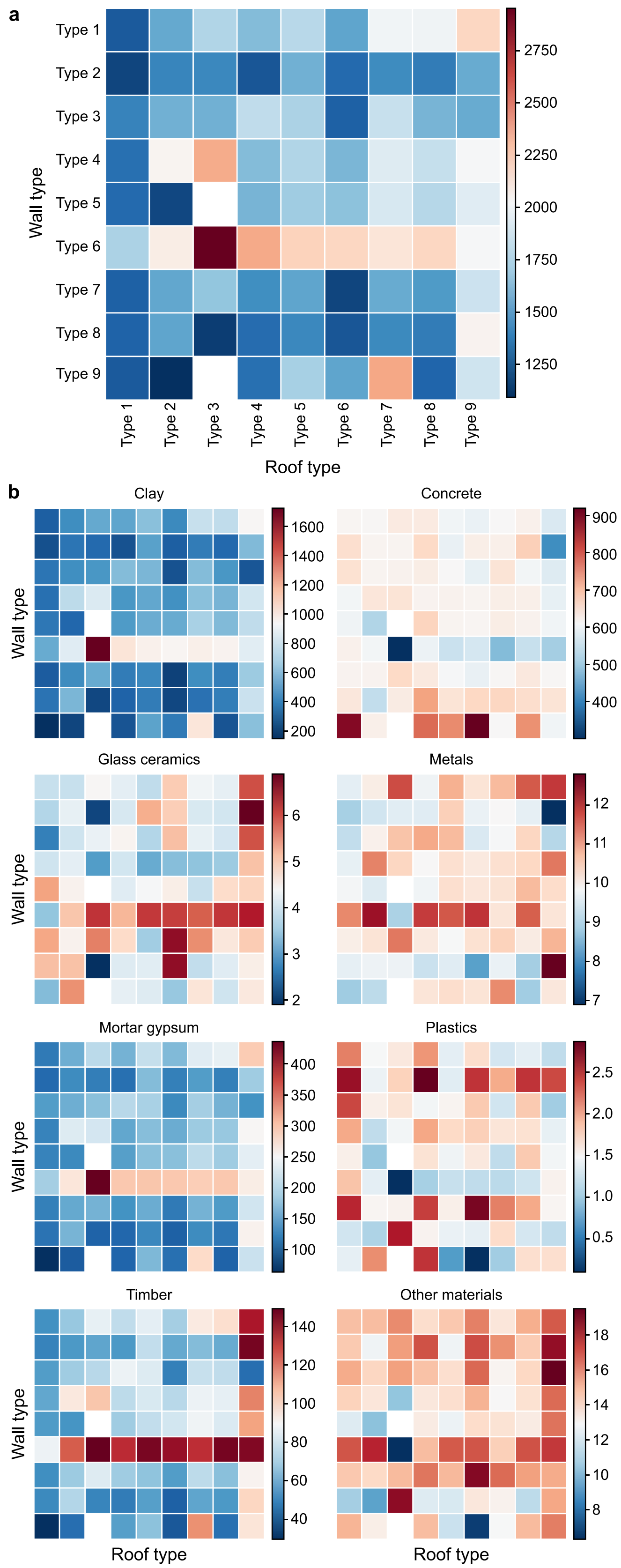

Fig. 7. Analysis of material intensity coefficient of residential buildings with different combinations of wall and roof types. **a**, The total material intensity coefficient under different combinations. **b**, The number of different material types (clay, concrete, glass ceramic, metal, gypsum mortar, wood, and other materials) used for the corresponding combinations. Darker colors indicate higher material intensity values, reflecting the combination's concentration in building material use.

sustainability, providing robust support for developing environmentally friendly urban buildings.

CRediT authorship contribution statement

Kun Sun: Writing - Original Draft, Visualization, Validation, Software, Resources, Methodology, Investigation, Formal Analysis, Data Curation. **Qiaoxuan Li:** Validation, Methodology, Formal Analysis, Data Curation. **Qiance Liu:** Writing - Review & Editing, Formal Analysis, Data Curation. **Jinchao Song:** Writing - Review & Editing, Formal Analysis. **Menglin Dai:** Writing - Review & Editing, Validation. **Xingjian Qian:** Validation, Data Curation. **Srinivasa Raghavendra Bhuvan Gummidi:** Writing - Review & Editing, Validation. **Bailang Yu:** Supervision. **Felix Creutzig:** Writing - Review & Editing, Validation. **Gang Liu:** Writing - Review & Editing, Visualization, Validation, Supervision, Software, Resources, Project Administration, Methodology, Investigation, Funding Acquisition, Formal Analysis, Data Curation, Conceptualization.

Declaration of competing interest

The authors declare that they have no known competing financial interests or personal relationships that could have appeared to influence the work reported in this paper.

Acknowledgments

This work is financially supported by the National Natural Science Foundation of China (71991484, 71991480), the Fundamental Research Funds for the Central Universities of Peking University, the Independent Research Fund Denmark (iBuildGreen), the European Union under grant agreement No. 101056810 (CircEUlar), and the China Scholarship Council (202006730004 and 202107940001).

Appendix A. Supplementary data

Supplementary data to this article can be found online at https://doi.org/10.1016/j.ese.2025.100538.

References

[1] X. Zhong, M. Hu, S. Deetman, B. Steubing, H.X. Lin, G.A. Hernandez, C. Harpprecht, C. Zhang, A. Tukker, P. Behrens, Global greenhouse gas emissions from residential and commercial building materials and mitigation strategies to 2060, Nat. Commun. 12 (1 12) (2021) 1–10, https://doi.org/10.1038/s41467-021-26212-z, 2021.

[2] E. Elhacham, L. Ben-Uri, J. Grozovski, Y.M. Bar-On, R. Milo, Global human-made mass exceeds all living biomass, Nature 588 (2020) 442–444, https://doi.org/10.1038/s41586-020-3010-5.

[3] P. Berrill, E.J.H. Wilson, J.L. Reyna, A.D. Fontanini, E.G. Hertwich, Decarbonization pathways for the residential sector in the United States, Nat. Clim. Change 12 (8 12) (2022) 712–718, https://doi.org/10.1038/s41558-022-01429-y, 2022.

[4] IEA, Buildings. https://www.iea.org/reports/buildings, 2022.

[5] S.J. Davis, Z. Liu, Z. Deng, B. Zhu, P. Ke, T. Sun, R. Guo, C. Hong, B. Zheng, Y. Wang, O. Boucher, P. Gentine, P. Ciais, Emissions rebound from the COVID-19 pandemic, Nat. Clim. Change 12 (5 12) (2022) 412–414, https://doi.org/10.1038/s41558-022-01332-6, 2022.

[6] J.S. Kikstra, A. Vinca, F. Lovat, B. Boza-Kiss, B. van Ruijven, C. Wilson, J. Rogelj, B. Zakeri, O. Fricko, K. Riahi, Climate mitigation scenarios with persistent COVID-19-related energy demand changes, Nat. Energy 6 (12 6) (2021) 1114–1123, https://doi.org/10.1038/s41560-021-00904-8, 2021.

[7] S. Pauliuk, N. Heeren, P. Berrill, T. Fishman, A. Nistad, Q. Tu, P. Wolfram, E.G. Hertwich, Global scenarios of resource and emission savings from material efficiency in residential buildings and cars, Nat. Commun. 12 (2021), https://doi.org/10.1038/s41467-021-25300-4.

[8] N. Zhou, N. Khanna, W. Feng, J. Ke, M. Levine, Scenarios of energy efficiency and CO2 emissions reduction potential in the buildings sector in China to year 2050, Nat. Energy 3 (11 3) (2018) 978–984, https://doi.org/10.1038/s41560-018-0253-6, 2018.

[9] Y. Yu, V. Junjan, D.M. Yazan, M.-E. Iacob, A systematic literature review on Circular Economy implementation in the construction industry: a policy-

making perspective, Resour. Conserv. Recycl. 183 (2022) 106359, https://doi.org/10.1016/j.resconrec.2022.106359.
[10] T. Huang, F. Shi, H. Tanikawa, J. Fei, J. Han, Materials demand and environmental impact of buildings construction and demolition in China based on dynamic material flow analysis, Resour. Conserv. Recycl. 72 (2013) 91−101, https://doi.org/10.1016/J.RESCONREC.2012.12.013.
[11] M. Lanau, G. Liu, U. Kral, D. Wiedenhofer, E. Keijzer, C. Yu, C. Ehlert, Taking stock of built environment stock studies: progress and prospects, Environ. Sci. Technol. 53 (2019) 8499−8515, https://doi.org/10.1021/acs.est.8b06652.
[12] H. Tanikawa, S. Hashimoto, Urban stock over time: spatial material stock analysis using 4d-GIS, Build. Res. Inf. 37 (2009) 483−502, https://doi.org/10.1080/09613210903169394.
[13] J. Lederer, A. Gassner, F. Kleemann, J. Fellner, Potentials for a circular economy of mineral construction materials and demolition waste in urban areas: a case study from Vienna, Resour. Conserv. Recycl. 161 (2020) 104942, https://doi.org/10.1016/J.RESCONREC.2020.104942.
[14] A. Miatto, H. Schandl, L. Forlin, F. Ronzani, P. Borin, A. Giordano, H. Tanikawa, A spatial analysis of material stock accumulation and demolition waste potential of buildings: a case study of Padua, Resour. Conserv. Recycl. 142 (2019) 245−256, https://doi.org/10.1016/J.RESCONREC.2018.12.011.
[15] R. Ortlepp, K. Gruhler, G. Schiller, Material stocks in Germany's non-domestic buildings: a new quantification method, Build. Res. Inform. 44 (2015) 840−862, https://doi.org/10.1080/09613218.2016.1112096.
[16] M. Arora, F. Raspall, L. Cheah, A. Silva, Residential building material stocks and component-level circularity: the case of Singapore, J. Clean. Prod. 216 (2019) 239−248, https://doi.org/10.1016/j.jclepro.2019.01.199.
[17] H. Tanikawa, T. Fishman, K. Okuoka, K. Sugimoto, The weight of society over time and space: a comprehensive account of the construction material stock of Japan, 1945−2010, J. Ind. Ecol. 19 (2015) 778−791, https://doi.org/10.1111/JIEC.12284.
[18] A. Stephan, A. Athanassiadis, Towards a more circular construction sector: estimating and spatialising current and future non-structural material replacement flows to maintain urban building stocks, Resour. Conserv. Recycl. 129 (2018) 248−262, https://doi.org/10.1016/J.RESCONREC.2017.09.022.
[19] J. Lederer, J. Fellner, A. Gassner, K. Gruhler, G. Schiller, Determining the material intensities of buildings selected by random sampling: a case study from Vienna, J. Ind. Ecol. 25 (2021) 848−863, https://doi.org/10.1111/JIEC.13100.
[20] N. Heeren, T. Fishman, A database seed for a community-driven material intensity research platform, Sci. Data 6 (1 6) (2019) 1−10, https://doi.org/10.1038/s41597-019-0021-x, 2019.
[21] P. Gontia, C. Nägeli, L. Rosado, Y. Kalmykova, M. Österbring, Material-intensity database of residential buildings: a case-study of Sweden in the international context, Resour. Conserv. Recycl. 130 (2018) 228−239, https://doi.org/10.1016/J.RESCONREC.2017.11.022.
[22] S. Marinova, S. Deetman, E. van der Voet, V. Daioglou, Global construction materials database and stock analysis of residential buildings between 1970-2050, J. Clean. Prod. 247 (2020) 119146, https://doi.org/10.1016/J.JCLEPRO.2019.119146.
[23] D. Yang, J. Guo, L. Sun, F. Shi, J. Liu, H. Tanikawa, Urban buildings material intensity in China from 1949 to 2015, Resour. Conserv. Recycl. 159 (2020) 104824, https://doi.org/10.1016/J.RESCONREC.2020.104824.
[24] M. Lanau, G. Liu, Developing an urban resource cadaster for circular economy: a case of Odense, Denmark, Environ. Sci. Technol. 54 (2020) 4675−4685, https://doi.org/10.1021/acs.est.9b07749.
[25] B. Sprecher, T.J. Verhagen, M.L. Sauer, M. Baars, J. Heintz, T. Fishman, Material intensity database for the Dutch building stock: towards Big Data in material stock analysis, J. Ind. Ecol. 26 (2022) 272−280, https://doi.org/10.1111/JIEC.13143.
[26] A. Arceo, H.L. MacLean, S. Saxe, Material intensity in single-family dwellings: variability between locations, functional unit and drivers of material use in Toronto, Perth, and Luzon, Resour. Conserv. Recycl. 188 (2023) 106683, https://doi.org/10.1016/J.RESCONREC.2022.106683.
[27] A. Mollaei, N. Ibrahim, K. Habib, Estimating the construction material stocks in two canadian cities: a case study of Kitchener and Waterloo, J. Clean. Prod. 280 (2021) 124501, https://doi.org/10.1016/j.jclepro.2020.124501.
[28] T. Fishman, A. Mastrucci, Y. Peled, S. Saxe, B. van Ruijven, RASMI: global ranges of building material intensities differentiated by region, structure, and function, Sci. Data 11 (1 11) (2024) 1−16, https://doi.org/10.1038/s41597-024-03190-7, 2024.
[29] N. Heeren, S. Hellweg, Tracking construction material over space and time: prospective and geo-referenced modeling of building stocks and construction material flows, J. Ind. Ecol. 23 (2019) 253−267, https://doi.org/10.1111/jiec.12739.
[30] J. Lederer, J. Fellner, A. Gassner, K. Gruhler, G. Schiller, Determining the material intensities of buildings selected by random sampling: a case study from Vienna, J. Ind. Ecol. 25 (2021) 848−863, https://doi.org/10.1111/JIEC.13100.
[31] X. Vilaysouk, S. Saypadith, S. Hashimoto, Semisupervised machine learning classification framework for material intensity parameters of residential buildings, J. Ind. Ecol. (2021), https://doi.org/10.1111/JIEC.13174.
[32] R. Mao, Y. Bao, Z. Huang, Q. Liu, G. Liu, High-resolution mapping of the urban built environment stocks in beijing, Environ. Sci. Technol. 54 (2020) 5345−5355, https://doi.org/10.1021/acs.est.9b07229.
[33] C. Yeh, A. Perez, A. Driscoll, G. Azzari, Z. Tang, D. Lobell, S. Ermon, M. Burke, Using publicly available satellite imagery and deep learning to understand economic well-being in Africa, Nat. Commun. 11 (1 11) (2020) 1−11, https://doi.org/10.1038/s41467-020-16185-w, 2020.
[34] H. Haberl, D. Wiedenhofer, F. Schug, D. Frantz, D. Virág, C. Plutzar, K. Gruhler, J. Lederer, G. Schiller, T. Fishman, M. Lanau, A. Gattringer, T. Kemper, G. Liu, H. Tanikawa, S. van der Linden, P. Hostert, High-resolution maps of material stocks in buildings and infrastructures in Austria and Germany, Environ. Sci. Technol. 55 (2021) 3368−3379, https://doi.org/10.1021/acs.est.0c05642.
[35] X. Li, Urban remote sensing using ground-based street view images, Urban Remote Sens. (2021) 91−113, https://doi.org/10.1002/9781119625865.CH5.
[36] S. Touzani, J. Granderson, Open data and deep semantic segmentation for automated extraction of building footprints, Remote Sens. 13 (2021), https://doi.org/10.3390/rs13132578.
[37] F. Trevisiol, A. Lambertini, F. Franci, E. Mandanici, An object-oriented approach to the classification of roofing materials using very high-resolution satellite stereo-pairs, Remote Sens. 14 (2022) 849, https://doi.org/10.3390/RS14040849, 849 14 (2022).
[38] M. Sun, F. Zhang, F. Duarte, C. Ratti, Understanding architecture age and style through deep learning, Cities 128 (2022) 103787, https://doi.org/10.1016/J.CITIES.2022.103787.
[39] Y. Ogawa, C. Zhao, T. Oki, S. Chen, Y. Sekimoto, Deep learning approach for classifying the built year and structure of individual buildings by automatically linking street view images and GIS building data, IEEE J. Sel. Top. Appl. Earth Obs. Rem. Sens. 16 (2023) 1740−1755, https://doi.org/10.1109/JSTARS.2023.3237509.
[40] K. Khumvongsa, J. Guo, S. Theepharaksapan, H. Shirakawa, H. Tanikawa, Uncovering urban transportation infrastructure expansion and sustainability challenge in Bangkok: insights from a material stock perspective, J. Ind. Ecol. 27 (2023) 476−490, https://doi.org/10.1111/JIEC.13342.
[41] D. Yang, M. Dang, J. Guo, L. Sun, R. Zhang, F. Han, F. Shi, Q. Liu, H. Tanikawa, Spatial−temporal dynamics of the built environment toward sustainability: a material stock and flow analysis in Chinese new and old urban areas, J. Ind. Ecol. 27 (2023) 84−95, https://doi.org/10.1111/JIEC.13335.
[42] X. Sun, B. Wang, Z. Wang, H. Li, H. Li, K. Fu, Research progress on few-shot learning for remote sensing image interpretation, IEEE J. Sel. Top. Appl. Earth Obs. Rem. Sens. 14 (2021) 2387−2402, https://doi.org/10.1109/JSTARS.2021.3052869.
[43] J. Li, X. Huang, J. Gong, Deep neural network for remote-sensing image interpretation: status and perspectives, Natl. Sci. Rev. 6 (2019) 1082−1086, https://doi.org/10.1093/NSR/NWZ058.
[44] X. Sun, D. Yin, F. Qin, H. Yu, W. Lu, F. Yao, Q. He, X. Huang, Z. Yan, P. Wang, C. Deng, N. Liu, Y. Yang, W. Liang, R. Wang, C. Wang, N. Yokoya, R. Hänsch, K. Fu, Revealing influencing factors on global waste distribution via deep-learning based dumpsite detection from satellite imagery, Nat. Commun. 14 (1 14) (2023) 1−13, https://doi.org/10.1038/s41467-023-37136-1, 2023.
[45] P. Ma, S. Petridis, M. Pantic, Visual speech recognition for multiple languages in the wild, Nat. Mach. Intell. 4 (11 4) (2022) 930−939, https://doi.org/10.1038/s42256-022-00550-z, 2022.
[46] S. Feng, H. Sun, X. Yan, H. Zhu, Z. Zou, S. Shen, H.X. Liu, Dense reinforcement learning for safety validation of autonomous vehicles, Nature 615 (7953 615) (2023) 620−627, https://doi.org/10.1038/s41586-023-05732-2, 2023.
[47] X. Yuan, J. Shi, L. Gu, A review of deep learning methods for semantic segmentation of remote sensing imagery, Expert Syst. Appl. 169 (2021) 114417, https://doi.org/10.1016/J.ESWA.2020.114417.
[48] Z. Zheng, Y. Zhong, J. Wang, A. Ma, L. Zhang, FarSeg++: foreground-aware relation network for geospatial object segmentation in high spatial resolution remote sensing imagery, IEEE Trans. Pattern Anal. Mach. Intell. 45 (2023) 13715−13729, https://doi.org/10.1109/TPAMI.2023.3296757.
[49] Z. Yao, Y. Lum, A. Johnston, L.M. Mejia-Mendoza, X. Zhou, Y. Wen, A. Aspuru-Guzik, E.H. Sargent, Z.W. Seh, Machine learning for a sustainable energy future, Nat. Rev. Mater. 8 (3 8) (2022) 202−215, https://doi.org/10.1038/s41578-022-00490-5, 2022.
[50] C.Y. Hsu, W. Li, Explainable GeoAI: can saliency maps help interpret artificial intelligence's learning process? An empirical study on natural feature detection, Intern. J. Geograph. Infor. Sci. 37 (2023) 963−987, https://doi.org/10.1080/13658816.2023.2191256.
[51] A. Benz, C. Voelker, S. Daubert, V. Rodehorst, Towards an automated image-based estimation of building age as input for Building Energy Modeling (BEM), Energy Build. 292 (2023) 113166, https://doi.org/10.1016/J.ENBUILD.2023.113166.
[52] E.J. Hoffmann, Y. Wang, M. Werner, J. Kang, X.X. Zhu, Model fusion for building type classification from aerial and street view images, Remote Sens. 11 (2019), https://doi.org/10.3390/rs11111259.
[53] K. Zhao, Y. Liu, S. Hao, S. Lu, H. Liu, L. Zhou, Bounding boxes are all we need: street view image classification via context encoding of detected buildings, IEEE Trans. Geosci. Rem. Sens. 60 (2022), https://doi.org/10.1109/TGRS.2021.3064316.
[54] M. Dai, W.O.C. Ward, G. Meyers, D. Densley Tingley, M. Mayfield, Residential building facade segmentation in the urban environment, Build. Environ. 199 (2021), https://doi.org/10.1016/j.buildenv.2021.107921.
[55] Z. Fan, F. Zhang, B.P.Y. Loo, C. Ratti, Urban visual intelligence: uncovering hidden city profiles with street view images, Proc. Natl. Acad. Sci. USA 120 (2023) e2220417120, https://doi.org/10.1073/PNAS.2220417120/SUPPL_FILE/PNAS.2220417120.SAPP.PDF.
[56] D. Raghu, M.J.J. Bucher, C. De Wolf, Towards a 'resource cadastre' for a circular economy − urban-scale building material detection using street view imagery and computer vision, Resour. Conserv. Recycl. 198 (2023) 107140, https://

doi.org/10.1016/j.resconrec.2023.107140.
[57] B. Zhou, A. Lapedriza, A. Khosla, A. Oliva, A. Torralba, Places: a 10 million image database for scene recognition, IEEE Trans. Pattern Anal. Mach. Intell. 40 (2018) 1452−1464, https://doi.org/10.1109/TPAMI.2017.2723009.
[58] R.R. Selvaraju, M. Cogswell, A. Das, R. Vedantam, D. Parikh, D. Batra, Grad-CAM: visual explanations from deep networks via gradient-based localization, Int. J. Comput. Vis. 128 (2020) 336−359, https://doi.org/10.1007/S11263-019-01228-7/FIGURES/21.
[59] B. Zhou, A. Khosla, A. Lapedriza, A. Oliva, A. Torralba, Learning deep features for discriminative localization, in: IEEE Conference on Computer Vision and Pattern Recognition (CVPR), 2016, pp. 2921−2929, https://doi.org/10.1109/CVPR.2016.319. 2016-December (2016).
[60] L. Jiao, W. Gao, R. Bie, A. Umek, A. Kos, Golf Guided Grad-CAM: attention visualization within golf swings via guided gradient-based class activation mapping, Multimed. Tool. Appl. 83 (2024) 38481−38503, https://doi.org/10.1007/S11042-023-17153-4/FIGURES/17.
[61] M. Lanau, R. Mao, G. Liu, Cities as organisms: urban metabolism of the four main Danish cities, Cities 118 (2021) 103336, https://doi.org/10.1016/j.cities.2021.103336.
[62] M. Lanau, L. Herbert, G. Liu, Extending urban stocks and flows analysis to urban greenhouse gas emission accounting: a case of Odense, Denmark, J. Ind. Ecol. 25 (2021) 961−978, https://doi.org/10.1111/jiec.13110.
[63] Bygnings -og Boligregistret, (n.d.). https://bbr.dk/forside (accessed April 9, 2023).
[64] H. Haberl, D. Wiedenhofer, S. Pauliuk, F. Krausmann, D.B. Müller, M. Fischer-Kowalski, Contributions of sociometabolic research to sustainability science, Nat. Sustain. 2 (2019) 173−184, https://doi.org/10.1038/s41893-019-0225-2.
[65] World Bank, Urban Development Overview, (n.d.). https://www.worldbank.org/en/topic/urbandevelopment/overview (accessed April 9, 2023).
[66] F. Kleemann, J. Lederer, H. Rechberger, J. Fellner, GIS-based analysis of vienna's material stock in buildings, J. Ind. Ecol. 21 (2017) 368−380, https://doi.org/10.1111/jiec.12446.
[67] A. Stephan, A. Athanassiadis, Quantifying and mapping embodied environmental requirements of urban building stocks, Build. Environ. 114 (2017) 187−202, https://doi.org/10.1016/J.BUILDENV.2016.11.043.
[68] N. Milojevic-Dupont, F. Wagner, F. Nachtigall, J. Hu, G.B. Brüser, M. Zumwald, F. Biljecki, N. Heeren, L.H. Kaack, P.-P. Pichler, F. Creutzig, EUBUCCO v0.1: European building stock characteristics in a common and open database for 200+ million individual buildings, Sci. Data 10 (2023) 147, https://doi.org/10.1038/s41597-023-02040-2.